

# Range-constrained traffic assignment for electric vehicles under heterogeneous range anxiety

Zhandong Xu<sup>1</sup>, Yiyang Peng<sup>2</sup>, Guoyuan Li<sup>2</sup>, Anthony Chen<sup>\*2</sup>, and Xiaobo Liu<sup>1</sup>

<sup>1</sup>School of Transportation and Logistics, Southwest Jiaotong University, Chengdu, China

<sup>2</sup>Department of Civil and Environmental Engineering, The Hong Kong Polytechnic University, Kowloon, Hong Kong, China

October 4, 2023

## Abstract

This paper studied the range-constrained traffic assignment problem (RTAP), where heterogeneous range anxiety is considered among the driving population by electric vehicles (EVs). In order not to get stranded en-route, each EV driver is assumed to have his/her own driving range limit for being able to complete the trip. As a result, two types of multi-class RTAP can be defined through discrete or continuous distributed range anxiety. Given path-based side constraint structures, we proposed two variational inequality (VI) formulations for modeling discrete and continuous RTAPs, where the former is finite-dimensional according to a discrete number of user classes and the latter is infinite-dimensional accounting for an infinite number of user classes. We reformulate the continuous RTAP into finite-dimensional by merging adjacent EV drivers into one group. A unified path-based solution framework is developed to solve the two RTAPs, built upon the gradient projection algorithm. We design column generation and dropping schemes to adaptively maintain compact path sets and an inner equilibration strategy to accelerate convergence. Finally, a small network is used to examine the correctness and effectiveness of proposed models, and a large Winnipeg network is adopted to evaluate the impacts of stochastic driving range on network flows and computation costs. Numerical results provide compelling evidence of the outstanding superiority of the proposed algorithm, and show that EV drivers with heightened sensitivity towards range anxiety may contribute to the emergence of critical links experiencing severe congestion.

Keywords: range anxiety; electric vehicles; continuous multi-class; gradient projection

---

\*Corresponding author, E-mail: [anthony.chen@polyu.edu.hk](mailto:anthony.chen@polyu.edu.hk)

# 1 Introduction

Electric vehicles (EVs) hold many promises that shape the future of transportation, such as lower noise pollution, improving fuel economy and reducing greenhouse emissions (Burns, 2013). As reported by [Global EV Outlook 2021](#), EV market accounted for 4.6% global sales and occupied about 1% of the world stock in 2020, a 43% increase over 2019. A growing number of vehicle manufacturers worldwide have declared electrification targets for 2030 and beyond. *Range anxiety*, however, is considered to be one of the major psychological barriers to large-scale public implementation and adoption of EVs (Kassakian et al., 2013; Qiu and Du, 2023). **It is what an EV driver feels when the battery storage is insufficient, and the electricity charging sources are unavailable.** This sparks fears of getting stranded en-route without being able to reach his/her destination, which inevitably increases travel time, inconvenience, and mental stress to the journey. Although most daily commuting trips can be accomplished within the range of an EV today (Shi et al., 2019), range anxiety still occurs when facing long-distance trips due to limited battery capacity, especially in areas lacking well-planned charging infrastructure. With the continuously increasing penetration of EVs, providing an efficient methodological tool to evaluate range anxiety is critical for EV traffic planning.

**The range anxiety issue has been widely studied in the literature due to its importance in various EV-related applications. For example, many have studied charge station location problems to alleviate range anxiety (e.g., see He et al., 2018; Wang et al., 2019; Xu et al., 2020a; Li et al., 2022). Liao et al. (2019) quantified consumer preferences to address the barrier of range anxiety. Huo et al. (2020) proposed a data-driven optimization model to improve its efficiency and overall profit. Zhang et al. (2021) empirically explored how fast charging affects range anxiety based on 1.7 million charging and driving records for EVs in Beijing. Wu and Kontou (2022) allocated rebates and charging infrastructure investments to promote EV adoption and meet emission reduction targets.**

In transportation studies, range anxiety is generally modeled as the maximum driving range or driving distance restriction imposed on EV drivers. It could be quantified by the self-perceived comfortable driving ranges, which substantially rest on stress-buffering personality and coping skills (Franke et al., 2012). Since the driving range varies with EV drivers, the range anxiety among the travel population should be characterized by a random distribution (Xie et al., 2017, 2019). Modeling EV drivers' routing behavior while concerning user heterogeneity leads to the so-called multi-class *Range-constrained Traffic Assignment Problem (RTAP)*. As a result, two types of multi-class RTAP are considered in this study through *discrete* or *continuous* distributions of range anxiety among EV drivers. The former is defined based on a discrete set of driving range limits, while the latter is more general to consider a continuous distribution among the driving population. The objective of this study is to present general equilibrium models and develop an efficient solution algorithm for multi-class RTAP with heterogeneous range anxiety.

## 1.1 Related studies

Below, we review three areas of recent works that are highly relevant to RTAP concerned in this paper. **Specifically, we first review side-constrained traffic assignment problems, this is followed by the continuous and discrete multi-class traffic assignment problems. The gradient projection (GP) algorithm developed in this study is discussed in the final subsection.**

### 1.1.1 Side-constrained traffic assignment

The standard traffic assignment problem (Beckmann et al., 1956) has been extended with additional constraints to address non-standard applications, referred to as the side-constrained traffic assignment problem (Larsson and Patriksson, 1995; Chen et al., 2011). One typical application is RTAP considered in this study, in which side constraints are the driving range limits of EV drivers imposed on paths between an origin and destination (O-D) pair (Jiang et al., 2012; He et al., 2014).

Another typical application with side constraints is the capacitated traffic assignment problem (CTAP), in which a rigid upper bound flow is imposed on a link to account for link capacity (Nie et al., 2004; Feng et al., 2020). Also, there are variants of CTAPs, e.g., combined distribution and assignment (Ryu et al., 2014) and transit assignment (Li and Chen, 2023). Noteworthy two critical distinctions exist between RTAP and CTAP. Firstly, the additional constraints of the former are exogenously defined based on the individual's fear of range anxiety, while the latter is endogenously determined by total flows traversing on a link. Secondly, the presence of link capacity constraint destroys the Cartesian product structure of the feasible set in CTAP, while RTAP does not create such concern. Nevertheless, RTAP requires restricting the path set for associated EV drivers to ensure feasibility.

In addition, the  $N$ -path traffic assignment problem exhibits similar features with RTAP (Lin and Leong, 2014). It assumes that individuals have a limited path set from which they can choose paths from. The work was later extended to logit-based stochastic user equilibrium to consider perception errors (Liu et al., 2018). However, there is a lack of physical explanations for excluding particular paths from the users' full path set.

### 1.1.2 Continuous and discrete multi-class traffic assignment

As previously mentioned, we aim to address the user heterogeneity with respect to range anxiety among EV drivers, which results in a multi-class traffic assignment problem. Jiang et al. (2012, 2014) initially studied a single-class RTAP by applying the same distance limit to the entire network. To conduct trip chain analysis, Wang et al. (2016) later presented a multi-class user equilibrium model, in which the driving population is associated with a discrete set of driving range limits. However, user heterogeneity in the population is more realistic to be represented by a continuous distribution rather than by an individual or several discrete values. To this end, Xie et al. (2017) extended the work of Wang et al. (2016) at the trip chain level, while Xie et al. (2019) extended the work of Jiang et al. (2012) at the trip level, both of which belong to the continuous

multi-class traffic assignment problem for considering heterogeneous range anxiety. It is worth noting that the continuous RTAP involves a potentially infinite number of user classes, naturally adding more complexity to both modeling and computation than the discrete version.

Once continuous multi-class traffic assignment is mentioned, one may associate it with the well-known time-toll bi-criteria traffic assignment problem, where users heterogeneity is considered through the continuously distributed value of time (VOT) (Leurent, 1993; Dial, 1999a,b). More recently, Xu et al. (2023) considered an infinite number of user classes under non-additive cost structures for time and toll trade-off. As a counterpart, a traditional approach to deal with continuous VOT distribution is the discretization method. That is, the entire feasible VOT range is divided into several predetermined user classes, each corresponding to a class-specific VOT value and travel demand (Li et al., 2023). Although a discrete model may bring potential estimation errors and computational burdens (Dial, 1996), it still receives much attention due to its ease of representation (e.g., see Yang and Huang, 2004; Han and Yang, 2008).

What distinguishes two continuous multi-class problems is the different considerations of random variables within the model. The VOT in bi-criteria traffic assignment combines time and toll cost in a linear manner to form generalized travel times, which appears in the model's objectives (Marcotte, 1998). As for RTAP, the stochastic driving range is defined to restrict the model's constraint set so as to ensure the feasibility of users' path choices. Therefore, how to generate and manipulate feasible paths for an infinite number of EV user classes becomes a critical issue in RTAP.

### 1.1.3 Gradient projection algorithm

The gradient projection (GP) algorithm is a well-known successful path-based solver for the traffic assignment problem with both fixed demand (Jayakrishnan et al., 1994; Chen et al., 2002) and elastic demand (Ryu et al., 2014). By decomposing the original problem into O-D based sub-problems, GP allows to perform simple projections with modest computational efforts. Thanks to its ingenious algorithmic features, GP has been further adapted to solve various network equilibrium problems, e.g., CTAP (Nie et al., 2004), stochastic traffic assignment (Xu et al., 2012; Zhou et al., 2012), non-additive traffic assignment (Chen et al., 2012; Tan et al., 2022), continuous bi-criteria traffic assignment (Xie et al., 2021; Xu et al., 2023) and transit assignment (Xu et al., 2020b, 2022; Du and Chen, 2022). A recent study of Chen et al. (2020) adopted a parallel computing strategy to solve TAP based on the GP algorithm. Although these mentioned problems have reported promising results with GP, no existing studies have applied GP to RTAP. Therefore, designing an efficient algorithm built on GP shed light on dealing with large-scale RTAPs, which contributes to practice.

## 1.2 Contributions

This study focuses on evaluating impacts and computing network flows by accounting for stochastic range anxiety. Although RTAP has been extensively studied in the literature (Jiang

et al., 2012; Wang et al., 2016; Xie et al., 2017, 2021), there are still research gaps in terms of both modeling and solution methods. More specifically, previous studies added flow-distance complementary constraints to model range anxiety. As a result, an out-of-range cost is defined for a binding constraint, i.e., when the path length exceeds the distance limit. The dimensionality of a continuous RTAP model (Xie et al., 2017, 2019) may become infinity due to incorporating an infinite number of constraints. However, the inequality constraint can be removed as the path feasibility is flow-independently determined by its physical length. This observation allows simpler forms of the model formulation based on the fact that individuals are making route decisions toward the time-distance trade-off for both discrete and continuous RTAPs. In terms of the solution method, the Frank-Wolfe (FW) algorithm is widely adopted for solving RTAPs (Jiang et al., 2012; Wang et al., 2016; Xie et al., 2019). However, the link-based solution may lose path information for a path-constrained problem. On the other hand, FW failed to obtain high-quality solutions for its well-known sluggish convergence behavior. **A noteworthy exception can be found in Xie et al. (2017), where a path-based projected gradient algorithm was introduced and tested on a synthetic network with different types and forms of driving ranges. This study endeavors to leverage the aforementioned observations for designing an alternative path-based algorithm for addressing both discrete and continuous RTAPs under large-scale transportation networks.**

Specifically, We propose general variational inequality (VI) formulations for both discrete and continuous RTAPs. For the continuous RTAP to account for an infinite number of user classes, the original infinite-dimensional formulation is transformed into finite-dimensional by merging neighboring classes pertaining to the same feasible path set. **The major contribution of this study is the development of a unified path-based gradient projection algorithmic framework for solving both discrete and continuous RTAPs. We designed column generation and column dropping schemes to adaptively maintain a compact path set, and devised an inner equilibration strategy to accelerate convergence. We demonstrate the features and the solution correctness of RTAP using a small network. The impacts of range anxiety on network flows and the computational efficiency of the proposed algorithm are further examined using a large-scale Winnipeg network.**

The rest of this paper is structured as follows. Section 2 describes the problem statement with range anxiety for EVs. Section 3 presents the general formulation to model both discrete and continuous range anxiety. The proposed GP algorithm is presented in Section 4, followed by the numerical results on small and large networks in Section 5. The concluding remarks and future research directions are specified in Section 6.

## 2 Problem statement

This study intends to explore the impact of heterogeneous range anxiety on UE flow patterns in the EV era. The addressed problem is stated as follows: From the psychological perspective of EV drivers, range anxiety is evaluated as the fear of running out of electricity. In particular,

it is highly related to vehicles having an insufficient driving range to reach their destination (Maybury et al., 2022). To eliminate range anxiety, EV drivers sometimes must select a feasible route to ensure not to exceed the distance limit. As depicted in Figure 1, we elaborate four impact factors from the characteristics of drivers to cause heterogeneous range anxiety. Taking the "driving experience" as an example, a new EV driver may be more sensitive towards range anxiety, such that more discount on the nominal battery state is perceived, so he/she will pick a path with a shorter distance than an experienced driver.

In this study, we provide further specifications on heterogeneous range anxiety by considering the stochastic nature of the driving limit, which plays a crucial role in determining the viability of a selected route. To maintain generality, both discrete and continuous distributions can be employed to model the stochastic driving limit, thus capturing the diverse range of anxiety experienced by drivers. While the discrete case accommodates a finite number of user classes, the continuous case offers a more realistic representation by considering an infinite number of user classes.

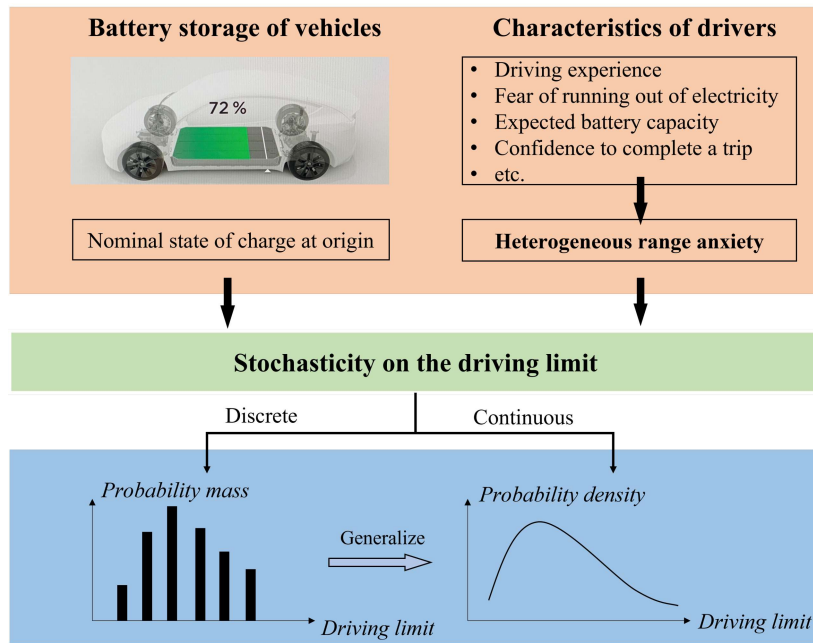


Figure 1: Illustration of the heterogeneity of comfortable distance limit

We proceed to discuss the route choice by taking into account discrete and continuous driving ranges. Suppose that an O-D pair is connected by three route alternatives (see Figure 2), each corresponding to a cost and distance. From the figure, we can discover several features for RTAPs, as detailed below:

(i) Path feasibility for a given user is deterministic thanks to the **flow-independent** path distance. As a result, the feasible path set for each class is also deterministic, as listed in the

associated boxes at the top of the subfigures.

(ii) For the continuously distributed driving range in Figure 2(b), the whole driving range support is split into three sub-ranges according to distances of "within paths" (i.e., Paths 2 and 3). Within a sub-range, two EV drivers with distinctive driving ranges can share the same feasible path set.

(iii) It turns out that individuals make route decisions toward the time-distance trade-off for both discrete and continuous RTAPs. Take the dominated path 3 as an example, users belonging to Class 3 or Sub-range 3 will not choose it because path 2 is more attractive to them.

As we shall see later, these observations will contribute to the development of both model formulations and solution algorithms for RTAPs.

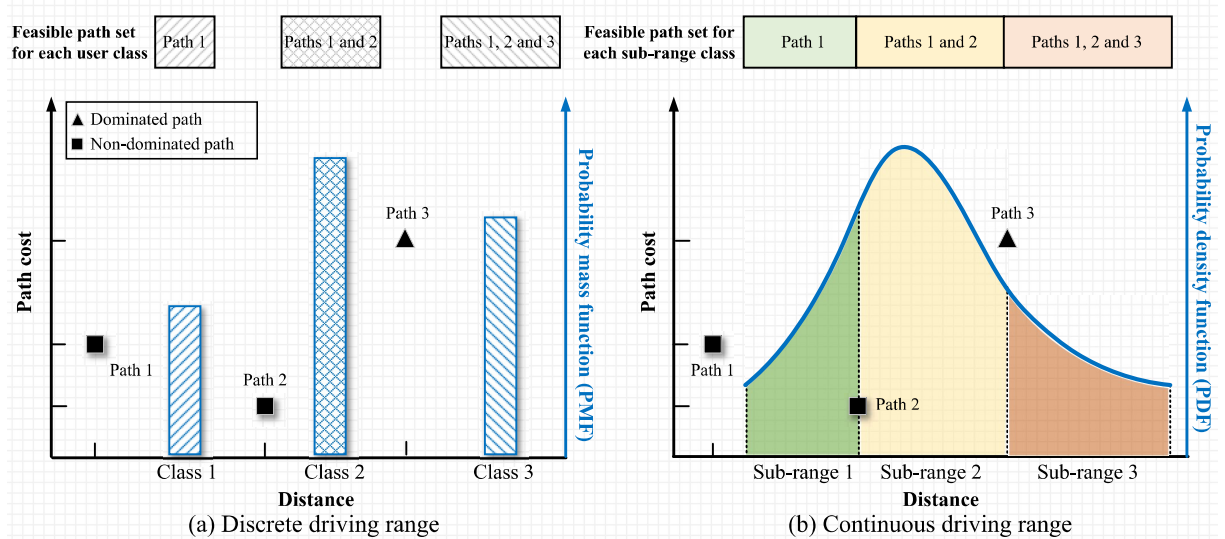


Figure 2: Route choices for discrete and continuous driving range.

If path disutility (cost) is flow-independent and paths are enumerated beforehand as shown in Figure 2, it is straightforward to determine which path should be chosen for any user with a given driving range. The equilibrium condition for users with stochastic range anxiety can be stated as below:

**Definition 1 (UE).** *At UE for any O-D pair, no EV driver can decrease his or her travel cost by unilaterally switching to an alternative route such that its length doesn't exceed the driving range.*

### 3 Formulations

Consider a network represented as a directed graph  $G(N, A)$ , where  $N$  and  $A$  denote the sets of nodes and links, respectively. Each link  $a \in A$  consists of two attributes, i.e., link travel time  $t_a(\cdot)$  and link travel distance  $d_a$ . In this paper, we assume that  $t_a(\cdot)$  is a positive, continuously

differentiable, and non-decreasing function with respect to flows on network links, while the link travel distance  $d_a$  is assumed to be a positive real number. Let  $W$  denote the set of O-D pairs,  $K^w$  the set of simple paths between O-D pair  $w \in W$ ,  $f_k$  the flow on path  $k \in K^w$ . The path travel time  $c_k$  and path distance  $d_k$  are, respectively, the sum of the time and length of each link belonging to the path, i.e.,

$$c_k = \sum_{a \in A} \delta_{a,k} t_a, \quad \forall k \in K^w, w \in W, \quad (1a)$$

$$d_k = \sum_{a \in A} \delta_{a,k} d_a, \quad \forall k \in K^w, w \in W, \quad (1b)$$

where  $\delta_{a,k} = 1$  if path  $k$  passes link  $a$ , and 0 otherwise.

The total flow on link  $a$  can be expressed as the function of all path flows passing through link  $a$ , i.e.,

$$x_a = \sum_{w \in W} \sum_{k \in K^w} \delta_{a,k} f_k, \quad \forall a \in A. \quad (2)$$

In this section, we first present general formulations for the range-constrained traffic assignment problem (RTAP) with discrete and continuous range anxiety separately, followed by a discussion of model properties.

### 3.1 Discrete range anxiety

To consider EV drivers' heterogeneity of range anxiety, it is assumed that there is a discrete set of range limits among the driving population. Additional notations are first introduced to model the discrete RTAP. Let  $M^w$  denote the set of discrete user classes of O-D pair  $w$ , each class  $m \in M^w$  corresponding to a given distance limit  $\theta_m^w (> 0)$  and a number of trips  $q_m^w$  associated with O-D pair  $w$ . We use  $K_m^w \subseteq K^w$  to represent the set of feasible paths in which the path length does not exceed the distance limit for user class  $m$  of O-D pair  $w$ , i.e.,  $K_m^w = \{k | k \in K^w, d_k \leq \theta_m^w\}$ . The class path-flow is denoted by  $f_{m,k}$ , which refers to the flow on path  $k \in K_m^w$  of class  $m$ . Accordingly, we have the following relationship:

$$f_k = \sum_{m \in M} f_{m,k}, \quad \forall k \in K^w. \quad (3)$$

The class path-flow must also satisfy flow conservation and non-negative constraints, i.e.,

$$\sum_{k \in K_m^w} f_{m,k} = q_m^w, \quad \forall w \in W, m \in M^w, \quad (4a)$$

$$f_{m,k} \geq 0, \quad \forall w \in W, m \in M^w, k \in K_m^w. \quad (4b)$$

According to Definition 1, the solution of discrete RTAP can be characterized by the following UE conditions

$$c_k \begin{cases} = u_m^w, & \text{if } f_{m,k} > 0 \\ \geq u_m^w, & \text{if } f_{m,k} = 0 \end{cases} \quad \forall w \in W, m \in M^w, k \in K_m^w, \quad (5)$$

where  $u_m^w$  is the minimum cost incurred by user class  $m$  traveling between O-D pair  $w$ .

For simplicity, we state the feasible set of discrete RTAP as  $\Omega_s \triangleq \{\mathbf{f}_s | \mathbf{q} = \Lambda \mathbf{f}_s, \mathbf{f}_s \geq \mathbf{0}\}$ , where  $\Lambda$  is the incidence matrix that links paths to O-D pairs,  $\mathbf{q} = \{q_m^w\}$  is the vector of class O-D demands, and  $\mathbf{f}_s = \{f_{m,k}\}$  is the vector of class path-flows. Given the above definitions, a variational inequality (VI) formulation is presented as follows.

**Proposition 1.** *A class path-flow vector  $\mathbf{f}_s^* = \{f_{m,k}^*\} \in \Omega_s$  satisfies the UE condition (5) if and only if  $\mathbf{f}_s^*$  is the solution to the following VI formulation, i.e., finding  $\mathbf{f}_s^* \in \Omega_s$  such that:*

$$\sum_{w \in W} \sum_{m \in M^w} \sum_{k \in K_m^w} c_k(\mathbf{f}_s^*) \cdot (f_{m,k} - f_{m,k}^*) \geq 0, \quad \forall \mathbf{f}_s \in \Omega_s, \quad (6)$$

where  $c_k(\mathbf{f}_s^*)$  is the travel cost on path  $k$  given  $\mathbf{f}_s^*$ .

### 3.2 Continuous range anxiety

This section further models the RTAP with continuous range anxiety across the driving population. Instead of using a set of discrete user classes (i.e.,  $\{\theta_m^w, \forall m\}$ ) for O-D pair  $w$ , the driving range  $\theta$  is considered as a random variable that follows a given probability density function (PDF), denoted by  $h^w(\cdot)$ , which is a result of various physical and psychological influence factors (e.g., see Xie et al., 2017). Without loss of generality, we assume that  $\theta$  lies in a given closed interval  $\Phi^w = [\theta_{lb}^w, \theta_{ub}^w]$  such that  $\theta_{ub}^w > \theta_{lb}^w > 0$ . For an EV driver who travels between O-D pair  $w$  and has a driving range of  $\theta \in \Phi^w$ , it is straightforward to define the associated feasible path set  $K_\theta^w$ , i.e.,  $K_\theta^w = \{k | k \in K^w, d_k \leq \theta\}$ .

As  $\theta$  belongs to a continuous support range, we adopt the concept of path-flow density  $\rho_k^w(\theta)$  used in Xie et al. (2017, 2019), which refers to the path-flow rate of user class  $\theta$  choosing a feasible path  $k \in K_\theta^w$  between O-D pair  $w$ . Therefore, the flow on path  $k$  can be written as

$$f_k = \int_{\theta_{lb}^w}^{\theta_{ub}^w} \rho_k^w(\theta) d\theta, \quad \forall k \in K^w, w \in W. \quad (7)$$

The feasible domain of  $\rho = \{\rho_k^w(\theta)\}$ , denoted by  $\tilde{\Omega}$ , should satisfy the following conditions:

$$\sum_{k \in K^w} \int_{\theta_{lb}^w}^{\theta_{ub}^w} \rho_k^w(\theta) d\theta = q^w, \quad \forall \theta \in \Phi^w, w \in W, \quad (8)$$

$$\rho_k^w(\theta) \geq 0 \quad \forall \theta \in \Phi^w, w \in W, \quad (9)$$

where  $q^w$  is the total number of trips of O-D pair  $w$ .

The solution of continuous RTAP can be characterized by the following UE conditions:

$$c_k \begin{cases} = u^w(\theta), & \text{if } \rho_k^w(\theta) > 0 \\ \geq u^w(\theta), & \text{if } \rho_k^w(\theta) = 0 \end{cases} \quad \forall w \in W, \theta \in \Phi^w, k \in K_\theta^w. \quad (10)$$

Next, we present an infinite-dimensional VI formulation for the continuous RTAP as below.

**Proposition 2.** An infinite class path-flow density vector  $\rho^* = \{\rho_k^{w*}(\theta)\}$  satisfies the UE condition (10) if and only if  $\rho^*$  is the solution to the following infinite-dimensional VI formulation, i.e., finding  $\rho^* \in \tilde{\Omega}$  such that:

$$\sum_{w \in W} \sum_{k \in K^w} \int_{\theta_{lb}^{w*}}^{\theta_{ub}^{w*}} c_k(\rho^*) \cdot [\rho_k^w(\theta) - \rho_k^{w*}(\theta)] d\theta \geq 0, \quad \forall \rho \in \tilde{\Omega}. \quad (11)$$

*Proof.* The proof can be completed by applying similar arguments following Appendix I in Marcotte and Zhu (1996).  $\square$

It can be seen that VI (11) is a direct extension from discrete VI (6) by generalizing the driving range to a continuous variable. Therefore, the continuous RTAP involves a potentially infinite number of user classes. While this formulation is straightforward and easy to understand, however, it contains an infinite number of decision variables, which could be impractical to solve the problem. In the following, we reformulate VI (11) as an equivalent finite-dimensional problem. The main idea stems from the recognition that two different users are actually "indistinguishable" if they share the same set of feasible paths. To see this, as shown in Figure 3, all users belong to  $[d_{k-1}, d_k)$  takes feasible path set from 1 to  $k-1$ , while users belong to  $[d_k, d_{k+1})$  takes from 1 to  $k$ . As a result, it is possible to merge adjacent EV drivers, but with the same set of feasible paths, into one group.

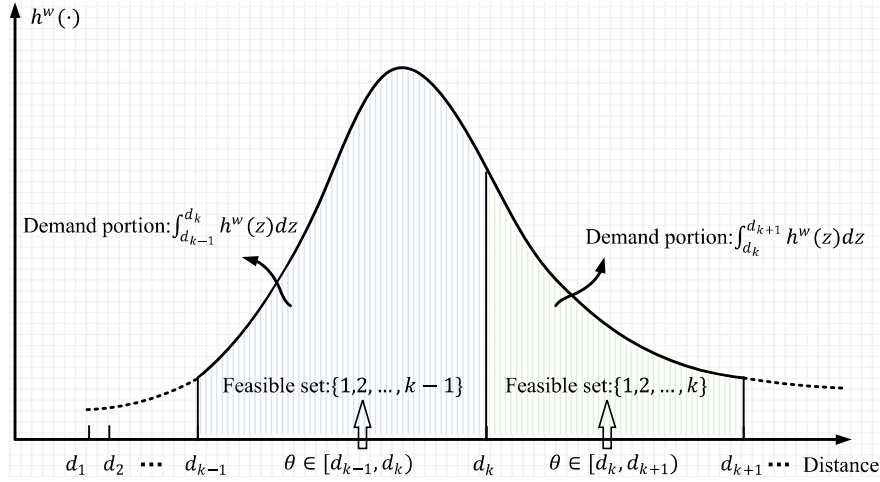


Figure 3: Illustration of the group merging according to the feasible path set.

To this end, we sort all paths in  $K^w$  in increasing order of  $d_k$  for any O-D pair  $w$ . Then, a fixed set of distance intervals within  $\Phi^w$  is defined as

$$\Phi_l^w = \begin{cases} [d_l^w, d_{l+1}^w), & \text{if } l = 1, \dots, |L^w| - 1 \\ (d_l^w, d_{l+1}^w], & \text{if } l = |L^w| \end{cases} \quad \forall w \in W, \quad (12)$$

where  $d_1^w = \theta_{lb}^w$ ,  $d_{|L^w|+1}^w = \theta_{ub}^w$ , and  $L^w$  is the set of sub-range groups of the divided interval. Thus,  $d_{l=2}^w$  represents the length of the first path that exceeds  $\theta_{lb}^w$ ,  $d_{l=3}^w$  the second one, and so on.

It is worth noting that users who lie into the same sub-range  $l$  take the same path set. Accordingly, let  $K_l^w$  denote the set of feasible paths that can be chosen by travelers within sub-range  $l$ , i.e.,  $K_l^w = \{k | k \in K^w, d_k \leq d_l^w\}$ . The class path-flow  $f_{l,k}$  is the flow on path  $k \in K_l^w$  within sub-range  $l$ . Then, we have the following relationship:

$$f_k = \sum_{l \in L^w} f_{l,k}, \quad \forall k \in K^w. \quad (13)$$

Because all EV drivers within sub-range  $l$  consider the same feasible path set, the UE condition (10) can be restated as follows:

$$c_k \begin{cases} = u_l^w, & \text{if } f_{l,k} > 0 \\ \geq u_l^w, & \text{if } f_{l,k} = 0 \end{cases} \quad \forall w \in W, l \in L^w, k \in K_l^w, \quad (14)$$

where  $u_l^w$  is the minimum cost incurred by sub-range  $l$  traveling between O-D pair  $w$ .

The class path-flows must also satisfy flow conservation and non-negative constraints, i.e.,

$$q_l^w = q^w \int_{d_l^w}^{d_{l+1}^w} h^w(z) dz = \sum_{k \in K_l^w} f_{l,k}, \quad \forall w \in W, l \in L^w, \quad (15)$$

$$f_{l,k} \geq 0, \quad \forall w \in W, l \in L^w, k \in K_l^w, \quad (16)$$

where  $q_l^w$  is the total number of trips for sub-range  $l$ .

Let  $\mathbf{f}_e = \{f_{l,k}\}$  denote the vector of class path-flows, and  $\Omega_e$  the feasible set based on Eqs. (15) and (16). Given the above definitions, a finite-dimensional VI formulation is presented as follows.

**Proposition 3.** *A class path-flow vector  $\mathbf{f}_e^* = \{f_{l,k}^*\} \in \Omega_e$  satisfies the UE condition (14) if and only if  $\mathbf{f}_e^*$  is the solution to the following VI formulation, i.e., finding  $\mathbf{f}_e^* \in \Omega_e$  such that:*

$$\sum_{w \in W} \sum_{l \in L^w} \sum_{k \in K_l^w} c_k(\mathbf{f}_e^*) \cdot (f_{l,k} - f_{l,k}^*) \geq 0, \quad \forall \mathbf{f}_e \in \Omega_e, \quad (17)$$

where  $c_k(\mathbf{f}_e^*)$  is the travel cost on path  $k$  given  $\mathbf{f}_e^*$ .

**Remark 1.** *Generally speaking, enumerating all paths is impractical, especially in large networks. In other words, it is computational expensive to predetermine sub-range set  $L^w$  for all  $w$ , despite having deterministic path length. To handle this problem, we will present column generation and dropping schemes to adaptively manage sub-range sets, as detailed in Section 4.*

### 3.3 Properties and discussion

Below, we discuss several properties of proposed models and present coherent relationships with existing formulations. First, we discuss about the solution existence and uniqueness for VI (6) and (17), respectively. If  $\mathbf{t}$  is a continuous function of link flows  $\mathbf{x}$ , then the path cost  $\mathbf{c}$  must also be continuous with respect to  $\mathbf{f}_s$  and  $\mathbf{f}_e$  by definition. Moreover, the feasible set  $\Omega_s$  and  $\Omega_e$  are non-empty, compact, and convex because it is a polyhedral. The existence of a solution then follows from Smith (1979). Next, we demonstrate the uniqueness of the total link flows.

**Theorem 1** (Uniqueness). *If  $\mathbf{t} = \{t_a(x_a)\}$  is strictly monotone with respect to  $\mathbf{x} = \{x_a\}$ , the total link flow solution  $\mathbf{x}^*$  is unique for VI (6) and (17).*

*Proof.* VI (6) can be transformed into an equivalent link-based VI, i.e., find  $\mathbf{x}^* \in \Omega_x$  such that:

$$\sum_{a \in A} t_a(\mathbf{x}^*) \cdot (x_a - x_a^*) \geq 0, \quad \forall \mathbf{x} \in \Omega_x, \quad (18)$$

where  $\Omega_x \triangleq \{\mathbf{x} | \mathbf{x} = \Delta \mathbf{f}_s, \mathbf{q} = \Lambda \mathbf{f}_s, \mathbf{f}_s \geq \mathbf{0}\}$ ,  $\Delta$  is the incidence matrix that maps path flows to link flows. The above transformation is also valid for VI (17). Given that  $\mathbf{t}$  is strictly monotone, the total link flows solution  $\mathbf{x}^*$  is unique.  $\square$

We further note that if  $t_a(\cdot), \forall a \in A$  is a positive, continuous, differentiable, and strictly increasing function of its own flow  $x_a$  (i.e., separable function), then VI (6) and (17) are equivalent to the well-known Beckmann's transformation:

$$\min_{\mathbf{f}} \sum_{a \in A} \int_0^{x_a = \sum_w \sum_{k \in K^w} \delta_{a,k} f_k} t_a(z) dz, \quad (19)$$

where feasible path flow vector  $\mathbf{f} = \{f_k\}$  is a function of multi-class flows to satisfy  $\Omega_s$  and  $\Omega_c$  for the discrete and continuous RTAP, respectively.

As each individual attempts to minimize his/her travel time while ensuring the route distance does not exceed the range limit, RTAP implicitly involves the time-distance bi-objective route choice embedded within the multi-class model. Consequently, we define (time-distance) weakly non-dominated paths as follows.

**Definition 2.** *Given a path flow pattern  $\mathbf{f}$ , path  $k$  between O-D pair  $w$  is said to be weakly non-dominated if there is no path  $k' \in K^w, k' \neq k$  such that  $c_{k'}(\mathbf{f}) < c_k(\mathbf{f})$  and  $d_{k'} \leq d_k$ .*

The above definition shows that there are no paths that are strictly shorter in time and no more distant than a weakly **non-dominated** path. The term "weakly" means that two different **non-dominated** paths can achieve equal travel times. To clarify, we proceed to provide a formal proof concerning the concept of weakly **non-dominated** paths.

**Lemma 1.** *At UE, for any O-D pair  $w$ , an EV driver with a higher driving range  $\theta_m^w$  will experience travel times that do not exceed those drivers with a smaller driving range  $\theta_{\bar{m}}^w$ , i.e.,  $u_m^w \leq u_{\bar{m}}^w$  for any  $\bar{m}$  such that  $\theta_m^w > \theta_{\bar{m}}^w$ .*

*Proof.* Suppose that there exist two user class  $m$  and  $\bar{m}$  such that  $u_m^w > u_{\bar{m}}^w$  and  $\theta_m^w > \theta_{\bar{m}}^w$  at UE. Consider a path  $k \in K_{\bar{m}}^w$  that carries positive flows, thus we have  $c_k = u_{\bar{m}}^w < u_m^w$  according to the UE condition. Since path  $k$  must also be included by  $K_m^w$  for class  $m$ , the relationship of  $c_k < u_m^w$  contradicts the UE condition for class  $m$ , which completes the proof.  $\square$

**Theorem 2.** *For any O-D pair  $w$ , EV drivers can only choose the path from the weakly non-dominated path set at UE.*

*Proof.* Given an equilibrium path flow pattern  $\mathbf{f}^*$ , let us consider an EV driver with  $\theta$  and chooses path  $k$  such that  $\theta \geq d_k$  and  $f_k^* > 0$ . Meanwhile, suppose there exists an unused path  $k'$  and it weakly dominates path  $k$  such that  $c_{k'}(\mathbf{f}^*) < c_k(\mathbf{f}^*)$  and  $d_{k'} \leq d_k$  as per Definition 2. Notably, path  $k'$  is also available to the driver, and in this case, path  $k'$  is more attractive since it has a shorter travel time. As a result, it leads to a contradiction to the UE condition since all EV drivers should experience minimum travel times under the range constraint. This implies that EV drivers can only choose the weakly non-dominated paths, which completes the proof.  $\square$

Figure 4 illustrates the relationship between proposed RTAP models and prior work. It is worthwhile to emphasize that if the driving range ( $\theta$ ) is sufficiently large, i.e., range anxiety no longer exists, RTAP then collapses to the standard TAP (Beckmann et al., 1956). To see this, each path  $k \in K^w$  is a feasible path choice for any user class  $\theta \in \Phi^w$ , leading to the standard UE condition. To consider multi-class range anxiety, existing studies add path flow-distance complementary constraints to the traditional flow conservation feasible set. Specifically, for the discrete RTAP model, Jiang et al. (2012) and Wang et al. (2016) defined range restriction constraint for each class  $m$ , i.e.,  $(\theta_m^w - d_k)f_k \geq 0$ . This inequality indicates that any path  $k$  whose length is shorter than the traveler's driving range cannot be used. Later, to consider the continuous RTAP, Xie et al. (2017) and Xie et al. (2019) introduced path flow density variable  $\rho_k^w(\theta)$  for extending the inequalities to infinite dimensional. As a result, it may lead to intractability as one theoretically needs to handle an infinite number of constraints. As outlined above, our proposed formulations can cover existing RTAP models in a much simpler form, which also enables us to design an efficient algorithm to solve RTAP.

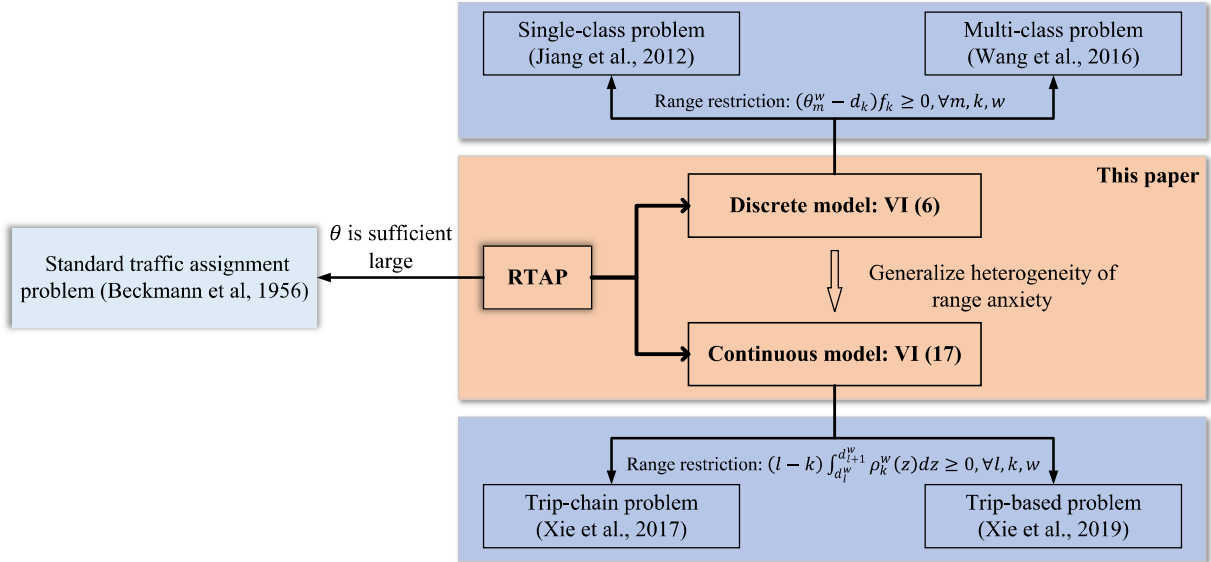


Figure 4: Relationship between proposed RTAP models and existing models.

## 4 Solution algorithm

This section presents a path-based gradient projection (GP) algorithm to solve both discrete and continuous RTAPs. Specifically, Section 4.1 begins by providing a unified framework of the proposed GP algorithm. Section 4.2 describes column generation schemes to include new potential paths in general networks. This is followed by GP operations for equilibration in Section 4.3. Section 4.4 describes the column dropping scheme during the solution process to keep the path set compact.

### 4.1 Unified framework

To efficiently solve RTAP, a unified GP framework that takes into account both discrete and continuous range anxiety is illustrated in Figure 5. Given network information (topology, link performance functions and demand) and range anxiety distributions (discrete or continuous), the unified procedure consists of five steps<sup>1</sup>, i.e., (1) initialization; (2) column generation; (3) flow equilibration; (4) column dropping; and (5) convergence test.

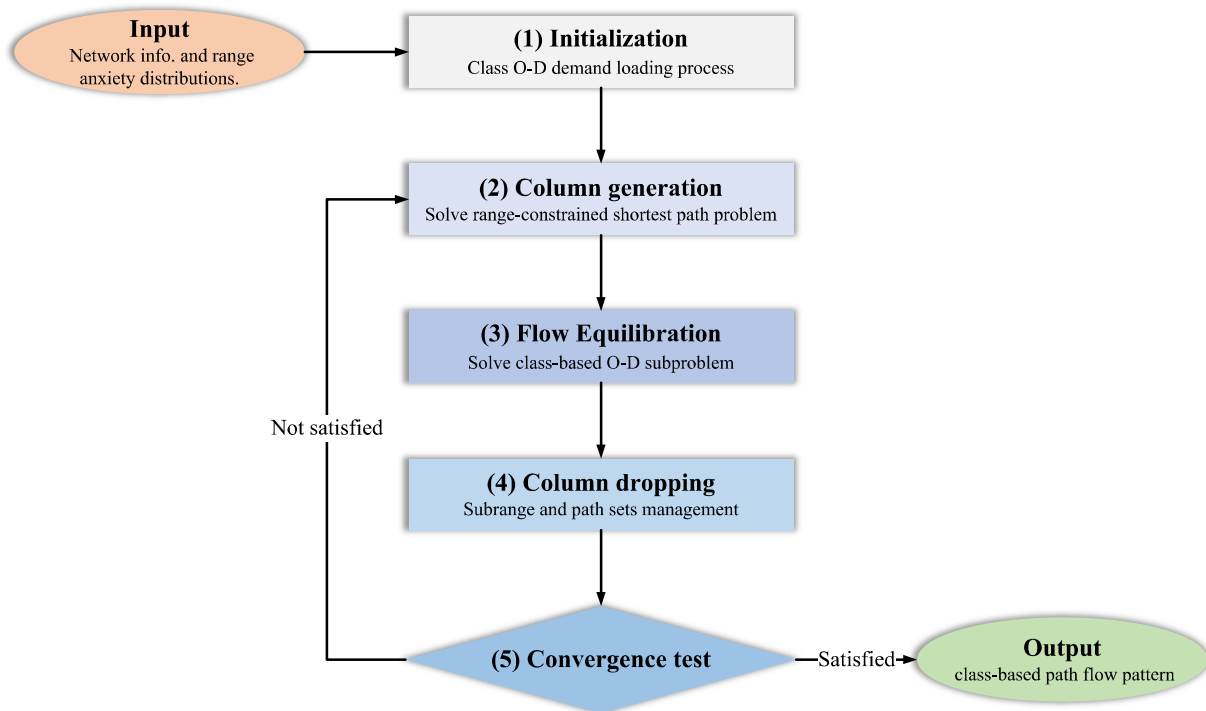


Figure 5: A unified framework of GP for solving RTAP.

First, the algorithm starts with loading class O-D demand to associated feasible and minimum-cost paths based on the zero-demand network. Second, the range-constrained shortest path prob-

<sup>1</sup>It is worth emphasizing that the link-based FW algorithm does not retain the generated minimum-cost paths in each iteration, and as a result, the column dropping operation is not needed. Furthermore, FW updates network link flows all-at-once by performing the all-or-nothing assignment and the line search at each iteration.

lem is solved to generate columns (variables) based on a bi-objective efficient path algorithm, as detailed in Section 4.2. Specifically, new potential and feasible paths are iteratively added into the working path set as needed. Third, the flow equilibration among range-feasible paths within a single O-D class is achieved by calling the GP solver, which is described in Section 4.3. Fourth, we eliminate the unused paths and merge adjacent sub-ranges for each O-D pair to keep the path set compact, as detailed in Section 4.4.

To measure how close the current solution is to the true UE conditions, the relative gap (RG) is used below,

$$RG = \begin{cases} 1 - \frac{\sum_{w \in W} \sum_{m \in M} u_m^w q_m^w}{\sum_{w \in W} \sum_{m \in M} \sum_{k \in K_m^w} f_{m,k} c_k} & \text{for discrete RTAP} \\ 1 - \frac{\sum_{w \in W} \sum_{l \in L} u_l^w q_l^w}{\sum_{w \in W} \sum_{l \in L} \sum_{k \in K_l^w} f_{l,k} c_k} & \text{for continuous RTAP.} \end{cases} \quad (20)$$

Fifth, we terminate the algorithm once the associated RG criteria or the maximum running time is reached, otherwise return to column generation. After termination, the proposed algorithm will output the equilibrium class-based path flow pattern.

## 4.2 Column generation

To avoid enumerating paths in RTAP, new paths are generated and added into the working set, only when they have (i) shorter distances than the associated driving range of EV drivers, and (ii) the potential to reduce the travel times within the path set. To this end, this section outlines a column generation scheme that solves the *range-constrained shortest path problem (RSPP)* at each iteration. Mathematically, we define the following RSPPs by fixing the path flow pattern:

- For the discrete range anxiety, given a class path-flow pattern  $\mathbf{f}_s$ , RSPP is defined as

$$\min \sum_{w \in W} \sum_{m \in M} \sum_{k \in K_m^w} c_k(\mathbf{f}_s) \cdot f_{m,k} \quad (21a)$$

$$s.t. \quad \text{Eqs. (4a)-(4b)}. \quad (21b)$$

- For the continuous range anxiety, given a class path-flow pattern  $\mathbf{f}_e$ , RSPP is written as

$$\min \sum_{w \in W} \sum_{l \in L^w} \sum_{k \in K_l^w} c_k(\mathbf{f}_e) \cdot f_{l,k} \quad (22a)$$

$$s.t. \quad \text{Eqs. (15)-(16)}. \quad (22b)$$

How to solve the above RSPPs for identifying a feasible path set for each user class that satisfies Conditions (i) and (ii) becomes the central concern. Recall that only time-distance non-dominated paths can be used when equilibrium is attained (see Theorem 2). Accordingly, we can identify non-dominated paths that achieve cost minimization for RSPPs. For completeness,

Appendix A describes the one-to-all label-setting time-distance non-dominated path-finding algorithm (Martins, 1984; Perederieieva et al., 2018). The basic idea is to store a non-dominated label set for each node, and iteratively add non-dominated labels or remove dominated labels based on the Dijkstra's algorithm (Dijkstra, 1959).

Algorithms 1 and 2 present detailed column generation procedures for the discrete and continuous RTAP, respectively. For the discrete problem, we will identify the optimal and feasible path for each predefined user class and add it into the working path set as needed (cf. Lines 6-9 in Algorithm 1).

---

**Algorithm 1** Column generation for the discrete RTAP

---

- 1: **Input:** Current path flow pattern  $\mathbf{f}_s = \{f_{m,k}\}$ .
  - 2: **for** each origin  $r$  **do**
  - 3:     Generate all non-dominated paths from origin  $r$  as per Appendix A.
  - 4:     **for** each destination  $s$  such that  $w = (r, s)$  **do**
  - 5:         Sort the non-dominated path set  $\bar{K}^w$  in descending order of  $d_k$ .
  - 6:         **for** each class  $m \in M^w$  **do**
  - 7:             Find path  $k = \operatorname{argmax}_{k'} \{d_{k'} \leq \theta_m^w | k' = 1, \dots, |\bar{K}^w|\}$ .
  - 8:             Set  $K_m^w = K_m^w \cup \{k\}$  if  $k \notin K_m^w$ .
  - 9:         **end for**
  - 10:     **end for**
  - 11: **end for**
  - 12: **Output:** Updated working path set  $K_m^w, \forall m, w$ .
- 

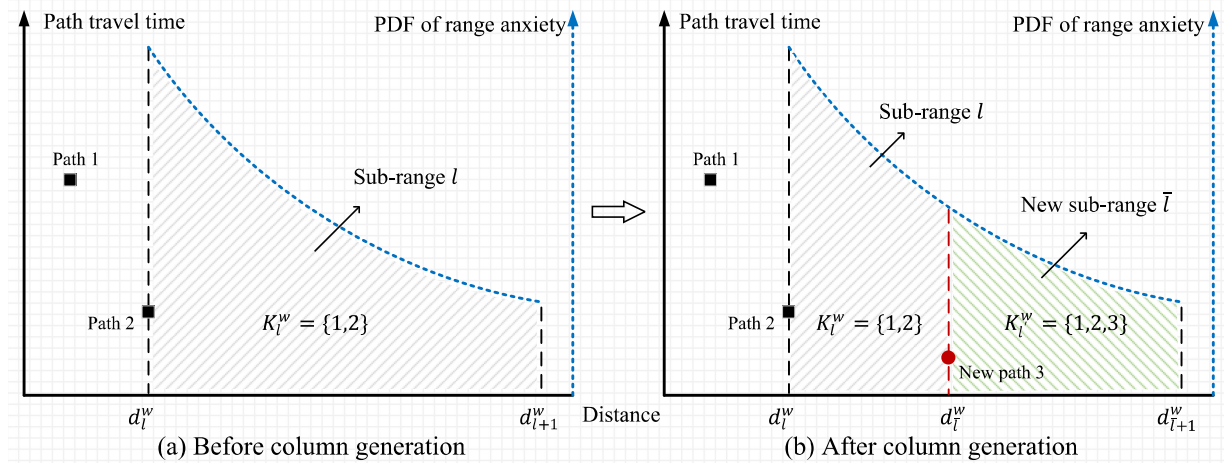


Figure 6: Illustration of column generation for continuous RTAP.

While the continuous problem is much more complicated because the sub-range set  $L^w$  must be dynamically managed when new paths are identified. Specifically, if the distance of an optimal

path  $k$  is shorter than the lower bound of range  $l$ , it can be directly added into  $K_l^w$  as needed (cf. Lines 7-8 in Algorithm 2). However, once  $d_k$  lies between  $d_l^w$  and  $d_{l+1}^w$ , we have to create a new sub-range  $\bar{l}$  and redistribute path flows and demand over  $l$  and  $\bar{l}$  (cf. Lines 9-15). To see this, Figure 6 provides a graphical illustration of the column generation for continuous RTAP. As shown in Figure 6(a), the original sub-range  $l$  has two feasible paths 1 and 2. Once a new path 3 is identified, the demand area is partitioned by sub-range  $l$  and new sub-range  $\bar{l}$ , where the new sub-range also includes path 3 (see Figure 6(b)). In other words, the user group in a continuous problem is dynamically maintained during the solution process, rather than being predetermined as in the discrete case.

---

**Algorithm 2** Column generation for the continuous RTAP

---

```

1: Input: Current path flow pattern  $\mathbf{f}_c = \{f_{l,k}\}$ .
2: for each origin  $r$  do
3:   Generate all non-dominated paths from origin  $r$  as per Appendix A.
4:   for each destination  $s$  such that  $w = (r, s)$  do
5:     for each sub-range  $l \in L^w$  in descending order of  $d_l^w$  do
6:       for each path  $k \in \bar{K}^w$  in descending order of  $d_k$  do
7:         if  $d_k \leq d_l^w$  and  $k = \operatorname{argmax}_{k'} \{d_{k'} \leq d_l^w\}$  then
8:           Set  $K_l^w = K_l^w \cup \{k\}$  if  $k \notin K_l^w$ .
9:         else if  $d_k > d_l^w$  and  $d_k < d_{l+1}^w$  then ▷ Range split
10:          Create a new sub-range  $\bar{l}$  such that  $d_{\bar{l}}^w = d_k$ ,  $d_{\bar{l}+1}^w = d_{l+1}^w$ , and add  $\bar{l}$  into  $L^w$ .
11:          Set  $K_{\bar{l}}^w = K_l^w \cup \{k\}$ ,  $f_{\bar{l},k} = 0$ ,  $q_{\bar{l}}^w = q^w \int_{d_k}^{d_{l+1}^w} h^w(z) dz$ .
12:          Update  $f_{\bar{l},k} = f_{l,k} \cdot \int_{d_k}^{d_{l+1}^w} h^w(z) dz / \int_{d_l^w}^{d_{l+1}^w} h^w(z) dz$  for all  $k \in K_{\bar{l}}^w$ .
13:          Update  $f_{l,k} = f_{l,k} \cdot \int_{d_l^w}^{d_k} h^w(z) dz / \int_{d_l^w}^{d_{l+1}^w} h^w(z) dz$  for all  $k \in K_l^w$ .
14:          Set  $d_{l+1}^w = d_k$ ,  $q_l^w = q^w \int_{d_l^w}^{d_{l+1}^w} h^w(z) dz$ .
15:         end if
16:       end for
17:     end for
18:   end for
19: end for
20: Output: Updated working path set  $K_l^w, \forall l, w$ .

```

---

### 4.3 Gradient projection

The main idea of the gradient projection (GP) algorithm is to simplify the constraint structure so that projection can be performed efficiently. More specifically, the "hard" constraints for discrete and continuous RTAP are the flow conservation conditions (4a) and (15) defined on each class-based path set, respectively. By **specifying a shortest** path  $\bar{k}$  under the current flow

pattern, the original feasible set can be redefined by non-negative constraints, which allows GP to perform simple projections on the non-negative orthant in each iteration (Jayakrishnan et al., 1994). Below, we present the flow update equations for both discrete and continuous RTAPs.

- For the discrete range anxiety at iteration  $n$ , path flows within class  $m$  are updated by

$$f_{m,k}(n+1) = \max\{0, f_{m,k}(n) - \mu(c_k - c_{\bar{k}})\}, \forall k \in K_m^w, k \neq \bar{k}, \quad (23a)$$

$$f_{m,\bar{k}}(n+1) = q_m^w - \sum_{k \in K_m^w, k \neq \bar{k}} f_{m,k}(n+1), \quad (23b)$$

where  $\mu$  is the stepsize.

- For the continuous range anxiety, path flows within sub-range  $l$  are updated by

$$f_{l,k}(n+1) = \max\{0, f_{l,k}(n) - \mu(c_k - c_{\bar{k}})\}, \forall k \in K_l^w, k \neq \bar{k}, \quad (24a)$$

$$f_{l,\bar{k}}(n+1) = q_l^w - \sum_{k \in K_l^w, k \neq \bar{k}} f_{l,k}(n+1). \quad (24b)$$

**Remark 2.** In Eqs. (23) and (24), the path travel time difference  $c_k - c_{\bar{k}}$  represents the descent search, while an appropriate stepsize  $\mu$  can be determined by the line search (e.g., Chen et al., 2012). Note that if the second derivative, i.e.,  $\frac{\partial(c_k - c_{\bar{k}})}{\partial f_{m,k}}$  or  $\frac{\partial(c_k - c_{\bar{k}})}{\partial f_{l,k}}$ , is not computationally expensive, we can directly use it as an automatic scaling (Jayakrishnan et al., 1994; Chen et al., 2002; Zhou et al., 2012; Ryu et al., 2014).

**Remark 3.** The flow update equations (23) and (24) in the GP algorithm outlined above consider all working paths at each iteration. For each non-shortest path  $k \neq \bar{k}$  as in Eq. (23a) or Eq. (24a), a quantity of  $\mu(c_k - c_{\bar{k}})$  units of flows are shifted to the current shortest path  $\bar{k}$  while ensuring non-negativity by max operator. Afterward, Eqs. (23b) and (24b) determine the exact flow on the shortest path  $\bar{k}$  to keep demand conservation for the discrete and continuous problem, respectively.

The detailed GP algorithm for a single O-D class subproblem is reported in Algorithm 3. We designed an adaptive inner loop strategy to accelerate convergence (cf. Lines 4-16). The equilibration operation is repeated until a convergence indicator ( $\Gamma < \gamma RG$ ) or maximum allowed inner loops ( $\eta$ ) is reached before naturally turning to column generation. This strategy has been shown to significantly accelerate the convergence of various traffic assignment problems (e.g., Chen and Jayakrishnan, 1998; Xu et al., 2020b, 2022; Tan et al., 2022; Xu et al., 2023).

To implement the strategy, a convergence indicator is defined as follows:

$$\Gamma = \begin{cases} 1 - \frac{q_m^w \cdot \min\{c_k\}}{\sum_{k \in K_m^w} c_k f_{m,k}} & \text{for the discrete RTAP} \\ 1 - \frac{q_l^w \cdot \min\{c_k\}}{\sum_{k \in K_l^w} c_k f_{l,k}} & \text{for the continuous RTAP,} \end{cases} \quad (25)$$

which is effectively a measure of the relative gap associated with the O-D class.

---

**Algorithm 3** GP algorithm for a single O-D class subproblem.

---

- 1: **Input:** The current class path-flow solution, control parameter  $\gamma$  and  $\eta$ .
  - 2: **Initialization:** Get path  $\bar{k} = k$  such that with lowest travel times. Set a counter  $\phi = 0$  and an indicator  $\nu = \text{TRUE}$  for the next inner loop.
  - 3: **Adaptive inner loop:** Lines 4-16.
  - 4: **while**  $\phi < \eta$  and  $\nu = \text{TRUE}$  **do**
  - 5:     Set  $\phi = \phi + 1$  and  $\nu = \text{FALSE}$ .
  - 6:     **for** each O-D pair  $w$  **do**
  - 7:         **for** each user class ( $m$  or  $l$ ) **do**
  - 8:             **if**  $\Gamma < \gamma RG$  **then** ▷ Solve the O-D subproblem
  - 9:                 Update class path-flows by Eq. (23) or (24).
  - 10:                 Update flows and costs of each affected link accordingly.
  - 11:                 Set  $\nu = \text{TRUE}$  if  $\nu = \text{FALSE}$ .
  - 12:                 Drop unused path  $k$  such that  $f_k = 0, \forall k \in K_{rs}$ .
  - 13:             **end if**
  - 14:         **end for**
  - 15:     **end for**
  - 16: **end while**
  - 17: **Output:** A new class path-flow solution.
- 

#### 4.4 Column dropping

In many variants of traffic assignment algorithms, column dropping is generally implemented to remove unused paths for keeping the path set compact. Just as in solving the discrete RTAP, we will drop the zero-flow class-based paths for each O-D pair, i.e.,  $f_{m,k} = 0$  for any  $m \in M$ ,  $k \in K_m^w$ ,  $w \in W$ . However, the continuous RTAP requires further considerations on merging adjacent sub-ranges as necessary.

Recall that in Figure 6, the sub-range set  $L$  is iteratively enlarged by splitting the range interval according to the newly added paths. During the solution process,  $|L^w|$  could become very large while some sub-ranges are redundant when they share the same path set. This would create computational burdens to flow equilibration as we have to solve additional subproblems. To see this, we provide a graphical illustration of the column dropping scheme, as shown in Figure 7. Before column dropping, suppose that we have three paths and two sub-ranges, in which path 3 is not utilized by any users anymore. As a result, we remove unused paths (i.e., path 3) and merge adjacent sub-ranges (i.e., sub-ranges  $l$  and  $l + 1$ ) after column dropping. Algorithm 4 presents the detailed column dropping procedure for the continuous RTAP.

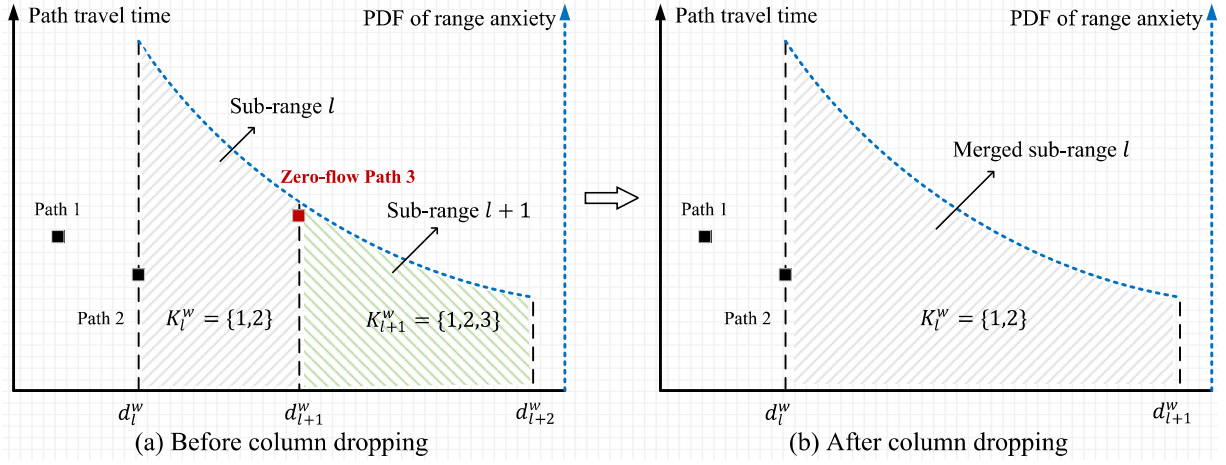


Figure 7: Illustration of column dropping for the continuous RTAP.

---

**Algorithm 4** Column dropping for the continuous RTAP

---

- 1: **Input:** Current sub-range set  $L^w, \forall w$  and working path set  $K_l^w, \forall l, w$ .
  - 2: **for** each O-D pair  $w \in W$  **do**
  - 3:   **for** each sub-range  $l \in L^w$  **do**  $\triangleright$  Drop unused paths
  - 4:     Remove  $k$  from path set  $K_l^w$  if  $f_{l,k} = 0$ .
  - 5:   **end for**
  - 6:   **for** each  $l \in L^w$  in descending order of  $d_l^w$  **do**  $\triangleright$  Merge adjacent sub-ranges if needed
  - 7:     Break the loop if  $l = 1$ .
  - 8:     Let  $l' = l - 1$ .
  - 9:     **if**  $K_l^w = K_{l'}^w$  **then**
  - 10:       Set  $d_{l'}^w = d_l^w, q_{l'}^w = q_{l'}^w + q_l^w$ .
  - 11:       **for** each path  $k \in K_{l'}^w$  **do**
  - 12:         Update  $f_{l',k} = f_{l',k} + f_{l,k}$ .
  - 13:       **end for**
  - 14:       Drop the unused sub-range  $l$  from set  $L^w$ .
  - 15:     **end if**
  - 16:   **end for**
  - 17: **end for**
  - 18: **Output:** Updated sub-range set  $L^w, \forall w$  and working path set  $K_l^w, \forall l, w$ .
-